

## Antiproton-deuteron annihilation into $\Lambda$ + anything below 1 GeV/c

M. A. Mandelkern, L. R. Price, J. Schultz, and D. W. Smith

Department of Physics, University of California, Irvine, California 92717

(Received 6 July 1982)

We present data on  $\Lambda$  production from two experiments in which the ANL 12-foot and the BNL 30-inch deuterium-filled bubble chambers were exposed to antiproton beams from 550 to 900 MeV/c. Some features of the data are compared to calculations of double scattering using  $\bar{K}$  and  $\bar{\Lambda}$  as the exchanged particles. The  $\Lambda$  final states in our experiments exhibit behavior which suggests that a double-scattering mechanism with a  $\bar{K}$  exchanged between the two nucleons is the most likely candidate for the  $\Lambda$  production mechanism. The data are compared with two other experiments in which  $\Lambda$  events are produced above the  $\bar{p}d \rightarrow \bar{\Lambda}\Lambda N$  threshold. A test of isospin invariance in these reactions is also reported.

### I. INTRODUCTION

Experiments<sup>1-3</sup> have reported enhanced  $\Lambda$  production resulting from  $\bar{p}d$  annihilation both in flight and at rest. It has been observed that  $\Lambda$ 's are produced much more frequently than  $\bar{\Lambda}$ 's above the  $\bar{p}d \rightarrow \bar{\Lambda}\Lambda N$  threshold. In contrast to the situation above threshold,  $\Lambda$  production below the  $\bar{p}d \rightarrow \bar{\Lambda}\Lambda N$  threshold can occur only if both nucleons of the deuteron participate in the process. Our study of the reaction



below the  $\bar{\Lambda}\Lambda N$  threshold (1180 MeV/c) is motivated by the apparently large cross section for reaction (1) and also by the possibility of observing baryonium states. Previous studies<sup>2,3</sup> of reaction (1) from 1 to 3 GeV/c have reported the  $\Lambda$  cross section to be  $\sim 400 \mu\text{b}$ . This is well above the measured<sup>4</sup>  $\bar{p}p \rightarrow \bar{\Lambda}\Lambda$  cross section of  $58 \pm 17 \mu\text{b}$  at 1.6 GeV/c and has stimulated investigations of mechanisms involving both nucleons of the deuteron in  $\bar{p}d$  annihilations leading to a  $\Lambda$ .<sup>2,3</sup> Camerini *et al.*<sup>2</sup> and Oh and Smith<sup>3</sup> have suggested that a double-scattering mechanism may describe the observed  $\Lambda$  production. The nature of the exchanged particle involved in the rescattering process has not been resolved because of the conflicting data reported from these two experiments. If the exchanged particle is an antibaryon, as suggested by Camerini *et al.*, then the search for  $\bar{B}B$  bound states becomes an exciting possibility.<sup>5</sup>

We present our data from reaction (1) and compare it to the two previous experiments. We also present results for  $\bar{\Lambda}$  and  $\bar{K}$  exchange mechanisms and compare them to the data.

### II. THE EXPERIMENT

The data reported here are based on a study of 80 000 pictures of antiprotons incident on the BNL 30-inch deuterium bubble chamber and 66 000 pictures of antiprotons incident on, and stopping in, the ANL 12-foot deuterium bubble chamber. The film in the BNL experiment was taken at three separate beam momenta with mean values of 552, 740, and 905 MeV/c at the chamber center. All the film in the ANL experiment was taken at one beam momentum measured to be 740 MeV/c at the window; the interaction momenta varied from 740 MeV/c to at rest. The incident momenta in the

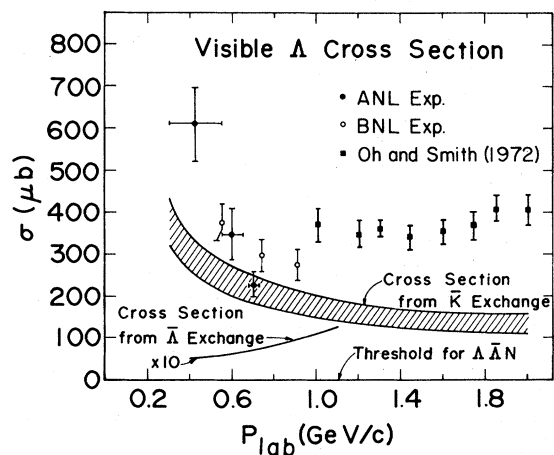


FIG. 1. The visible  $\Lambda$  cross sections in this experiment are compared with (a) the experiment of Oh and Smith (Ref. 3), (b) the cross section calculated from  $\bar{K}$  exchange, and (c) the cross section calculated from  $\bar{\Lambda}$  exchange.

TABLE I. Summary of data from the ANL and BNL experiments including visible  $\Lambda$  cross section and principal final states.

$P_{\text{beam}}$ (MeV/c)	ANL experiment			BNL experiment		
	300–550	550–650	650–725	552	740	905
No. of $\Lambda$ events	62	63	74	94	128	160
$\sigma_{\Lambda}(\text{visible})$ ( $\mu\text{b}$ )	$609 \pm 89$	$348 \pm 51$	$228 \pm 31$	$375 \pm 44$	$297 \pm 38$	$275 \pm 37$
Final states						
1. $\Lambda K^+ \pi^- \pi^0$	8	10	11	19	22	20
2. $\Lambda K^0 \pi^+ \pi^-$	9	8	12	17	17	25
3. $\Lambda K^+ \pi^+ \pi^- \pi^-$	2	2	7	9	13	8
4. $\Lambda K^+ \pi^+ \pi^+ \pi^- \pi^- \pi^0$	3	4	2	7	9	12
5. $\Lambda K^0 \pi^+ \pi^- \pi^0$	5	4	3	3	12	12
Subtotal <sup>a</sup>	31	36	41	59	79	85
Missing-mass fits	25	24	28	29	35	50
Other events <sup>b</sup>	6	3	5	6	14	25
Total number of $\Lambda$ events	62	63	74	94	128	160

<sup>a</sup>Includes other final states not listed above.

<sup>b</sup>Ambiguities and final states with  $\gamma$ -ray fits.

ANL film were divided into three momentum bins: 300–550 MeV/c, 550–650 MeV/c, and 650–725 MeV/c. Table I shows beam momenta and cross sections for the two experiments, as well as a breakdown of numbers of events found in the principal final states.

We measured all the  $V$  events, and approximately 20% of the film in both experiments was remeasured to determine the scanning efficiency. The events were processed through the TVGP-SQUAW programs and fit to final states including those shown in Table I. The cross sections obtained for reaction (1), not corrected for the neutral decay mode of the  $\Lambda$ , are shown in Fig. 1 along with the data of Oh and Smith.<sup>3</sup>

### III. DOUBLE SCATTERING

Since both nucleons are necessarily involved in the observed  $\Lambda$  production, it is likely that the production mechanism is a result of double scattering. Figure 2 shows examples of double scattering where the incoming antiproton interacts with the first nucleon (e.g., a proton) and creates a particle-antiparticle pair. The antiparticle interacts with the second nucleon of the deuteron to complete the process.

Figure 2(a) shows a  $\Lambda \bar{\Lambda}$  pair created at the first vertex and the  $\bar{\Lambda}$  interacting at the second vertex. The  $\bar{\Lambda}$  exchange diagram was suggested by Camerini *et al.* as the most likely mechanism for  $\Lambda$  production because of (i) the striking peripheral production of  $\Lambda$ 's observed in their data and (ii) a peak observed in the missing-mass distributions ( $\bar{p}d \rightarrow \Lambda + \text{MM}$ ) near the  $\Lambda \bar{N}$  threshold.

We have estimated the total  $\Lambda$  cross section and the missing-mass distribution for  $\bar{p}d \rightarrow \Lambda + \text{MM}$  based on the triangle diagram with  $\bar{\Lambda}$  exchange. The basic assumptions underlying this calculation and the results derived are described in Appendix A.

Figure 3 shows the result for  $d\sigma/dm_B$  for  $\bar{\Lambda}$  exchange normalized to our data. Here  $m_B$  is the

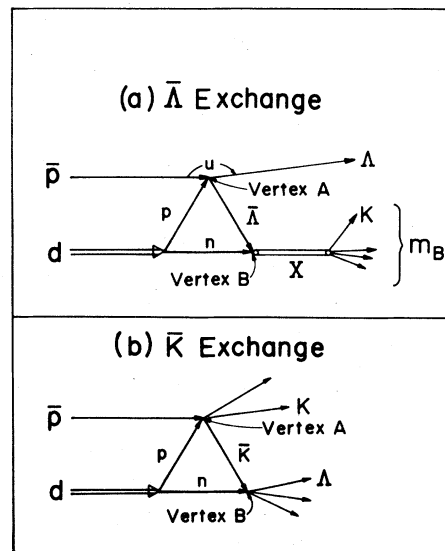


FIG. 2. Double-scattering diagrams: (a)  $\bar{\Lambda}$  exchange diagram where the observed  $\Lambda$  is produced at the first vertex and (b)  $\bar{K}$  exchange diagram where the observed  $\Lambda$  is produced at the second vertex. A hypothetical baryonium state  $X$  is illustrated in (a).

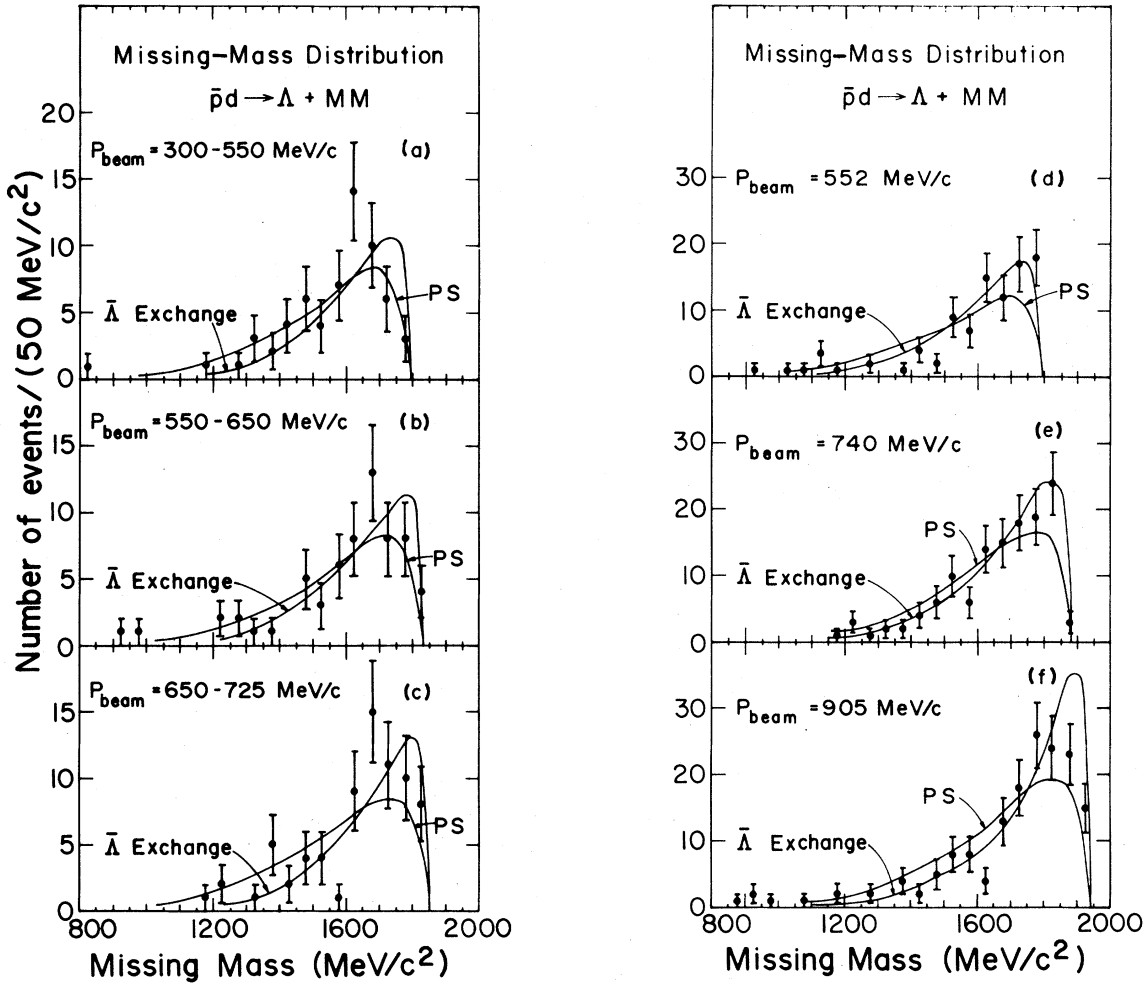


FIG. 3. Missing mass recoiling off the  $\Lambda$  in the reaction  $\bar{p}d \rightarrow \Lambda + MM$  for our six beam momenta. The phase space and  $\bar{\Lambda}$  exchange curves are normalized to the number of events.

mass of the system produced at vertex  $B$ , i.e., the missing mass in the process. In the same figure, the phase space is plotted for four-, five-, and six-body final states added together and weighted according to their respective branching ratios. Both calculated curves fit the data quite well; indeed, one could not choose the functional dependence of the exchange mechanism distribution over the phase-space distribution.

A serious deficiency of the  $\bar{\Lambda}$  exchange model is in the expected absolute  $\Lambda$  cross section shown in Fig. 1. The cross section due to  $\bar{\Lambda}$  exchange is very much smaller than the observed cross section. Although one might expect several other similar diagrams to contribute to the  $\Lambda$  production, the combined effect would probably still fall far short of the observed cross section. Furthermore, the calculated cross section increases with energy at low energy, in contrast to the data which appears to fall and then remain

essentially constant.

Figure 2(b) shows a  $\bar{K}K$  pair created at the first vertex. In principle, this  $\bar{K}$  exchange process can be estimated using the triangle diagram calculation as described in Appendix A for  $\bar{\Lambda}$  exchange. However, the  $\bar{K}$  exchange diagram does not yield directly the distribution of mass recoiling against the  $\Lambda$ ; for this one must introduce the momentum and angular distributions of  $\Lambda$ 's at the  $B$  vertex. Unfortunately there are several pertinent reactions which must be considered, for which the detailed distributions are not readily available.

The total cross section for  $\Lambda$  production by means of  $\bar{K}$  exchange can be estimated in a much more simple and direct fashion, since the triangle diagram can be viewed as a two-step process in which a "real"  $\bar{K}$  is produced at vertex  $A$  and interacts at vertex  $B$  to produce a  $\Lambda$ . To estimate the expected rate for this process, we write

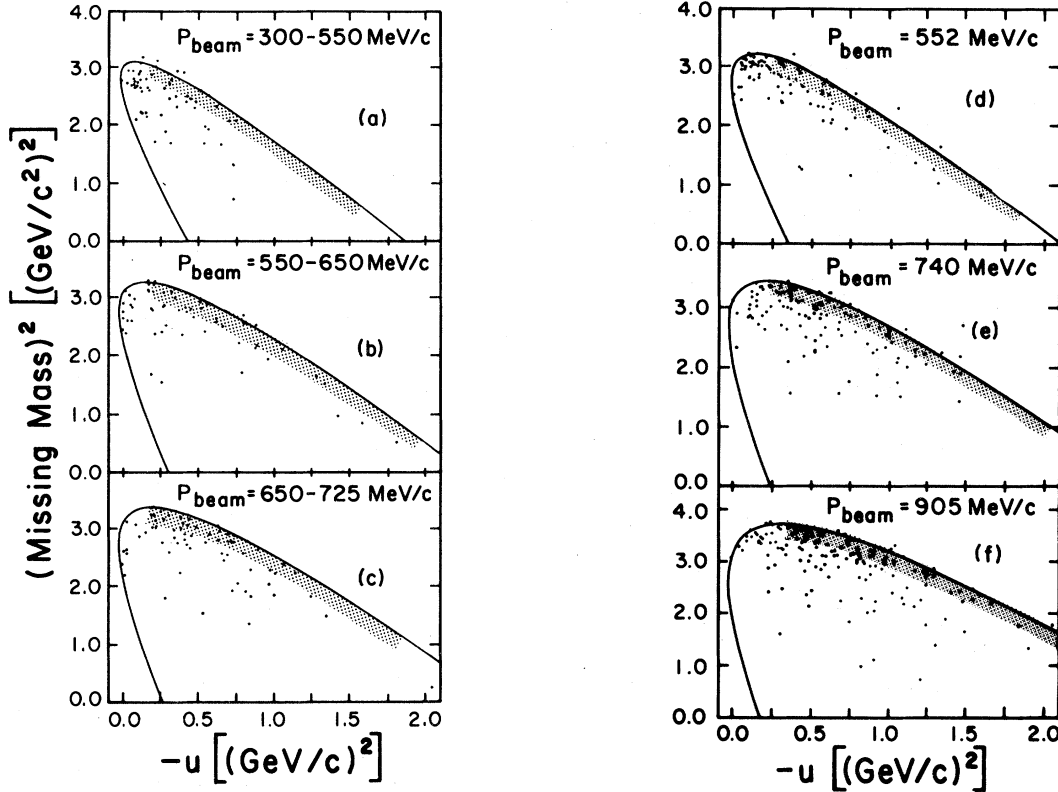


FIG. 4. Chew-Low plots of the missing mass squared recoiling off the  $\Lambda$  versus the momentum transfer  $u$ . The momentum transfer is shown in Fig. 2(a). The shaded area shows where an accumulation of events would occur if quasinuclear states were produced from  $\bar{\Lambda}$  exchange.

$$\begin{aligned} \sigma(\bar{p}d \rightarrow \Lambda K + \text{anything}) &\approx 2 \times \sigma(\bar{p}p \rightarrow \bar{K}K + \text{anything}) \times \text{probability}(\bar{K}N \rightarrow \Lambda + \text{anything}) \\ &= 2 \times \sigma(\bar{p}p \rightarrow \bar{K}K + \text{anything}) \frac{\sigma(\bar{K}N \rightarrow \Lambda + \text{anything})}{4\pi} \left\langle \frac{1}{r^2} \right\rangle_d. \end{aligned} \quad (2)$$

A factor of 2 is introduced to take into account both nucleons of the deuteron. The cross section for  $\bar{K}N \rightarrow \Lambda + \text{anything}$  obtained from  $K^-N$  experiments<sup>6</sup> is approximately 10 mb. The value<sup>1</sup> used for  $\langle r^{-2} \rangle_d / 4\pi$  is  $2.2 \times 10^{24} \text{ cm}^{-2}$ . From Eq. (2) we find that

$$\sigma(\Lambda) \approx 0.044 \sigma(\bar{p}p \rightarrow \bar{K}K + \text{anything}). \quad (3)$$

Using the branching ratio for visible  $\Lambda$  decays (64%), and data on  $\bar{K}K$  production we obtain the approximate result given by the hatched area of Fig. 1. The result is extrapolated to low energy assuming a  $1/P_{\text{lab}}$  behavior of the annihilation cross section. The estimate is in good agreement with the data.

A question of considerable current interest is the possibility of producing quasinuclear baryonium states via  $\bar{\Lambda}$  exchange. Bogdanova and Markushin<sup>5</sup> have suggested that production of strange quasinu-

clear  $\bar{\Lambda}N$  states might be observed in  $\bar{p}d$  interactions, with events concentrated on or near the boundary of a Chew-Low plot, in which the missing mass squared recoiling off the  $\Lambda$  is plotted against the momentum transfer  $u$ . Figure 4 shows our data on a Chew-Low plot with the kinematical boundary shown. The shaded area near the boundary is the physical region where one would expect candidates for quasinuclear states produced by  $\bar{\Lambda}$  exchange. No bands are seen, nor does there appear to be any significant accumulation of events in this region; events are consistent with phase space.

In general the  $u$  distribution is not in accord with  $\bar{p}p \rightarrow \Lambda\Lambda$ , a peripheral process favoring  $\Lambda$  production backward with respect to the incident  $\bar{p}$  direction. This should be reflected in the angular distribution of  $\Lambda$ 's in the  $\bar{p}d$  center-of-mass system. One of the arguments for  $\bar{\Lambda}$  exchange by Camerini *et al.*<sup>2</sup>

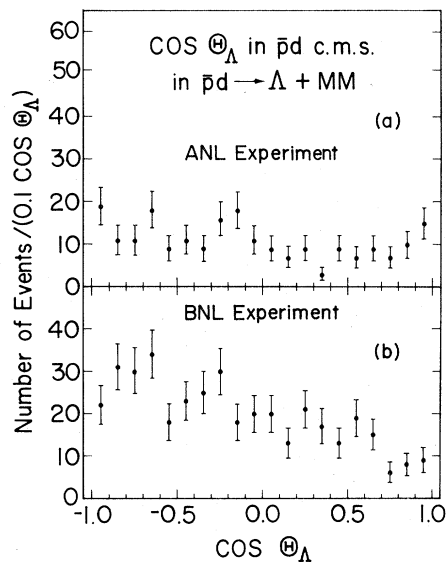


FIG. 5. Angular distribution of the  $\Lambda$  events in the  $\bar{p}d$  center-of-mass system, all beam momenta combined. Peripheral production of  $\Lambda$ 's resulting from  $\bar{\Lambda}$  exchange [Fig. 2(a)] is not observed.

was based on observed peripheral  $\Lambda$  production. The angular distribution of our  $\Lambda$  events in the  $\bar{p}d$  center-of-mass system is shown in Fig. 5. We do not observe any significant peripheral production at our energies.

Oh and Smith<sup>3</sup> have compared the transverse momentum distribution of the  $\Lambda$  with that expected from  $\bar{K}$  exchange based on a diffractive double-scattering model. In this case, a diffractive amplitude is used to describe the transverse momentum of the  $\bar{K}$  produced at vertex  $A$

$$F_1(p_{\bar{K}_t}) = A \exp(-ap_{\bar{K}_t}^2) \quad (4)$$

and another diffractive amplitude is used to describe the transverse momentum of the  $\Lambda$  produced at vertex  $B$

$$F_2(p_{\Lambda_t}) = B \exp(-bp_{\Lambda_t}^2), \quad (5)$$

where  $p_{\bar{K}_t}$  and  $p_{\Lambda_t}$  are the transverse momenta of the  $\bar{K}$  and  $\Lambda$ , respectively, and  $a$  and  $b$  are the diffractive parameters  $\approx 4.5 \text{ GeV}^{-2}$ . Similar diffractive amplitudes were used by Dean<sup>7</sup> to describe multiple scattering in deuteron targets in processes where only elastic scattering was considered. Although the use of such amplitudes for the annihilation process may not be justifiable, this model seems to fit the data reasonably well. In Fig. 6 we show the transverse momentum of the  $\Lambda$ 's using the diffractive amplitudes (4) and (5); reasonable agreement with

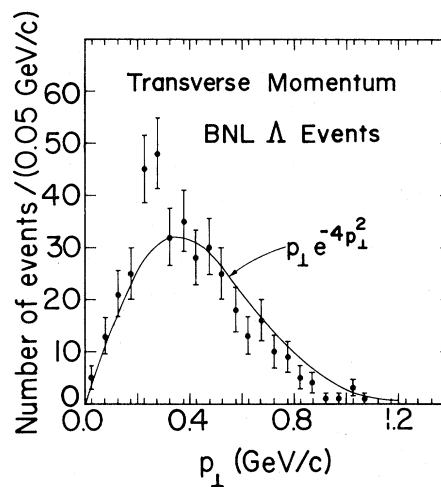


FIG. 6. Transverse momentum of the  $\Lambda$ 's in our BNL experiment. The curve is the diffractive amplitudes [Eqs. (4) and (5)] fit to our data.

the data is obtained.

From studies of annihilation at rest, Bizzarri *et al.*,<sup>1</sup> argue against a double-scattering hypothesis in favor of some intrinsic three-body annihilation mechanism. Their argument is based on the apparent absence of meson resonances in the final state; such resonances, they contend, would result from the  $\bar{N}N$  annihilation step in a rescattering process.

However, as indicated in Table I, the final states characteristically have two or more pions, each of which may originate from either vertex of the double scattering. This is particularly true of the  $\bar{K}$  exchange process of Fig. 2(b) in which the  $\bar{p}N$  annihilation at vertex  $A$  has a high probability of yielding several pions. In the mass combinations which comprise meson resonances (both pionic and kaonic) the inclusion of combinations involving particles from different vertices inevitably tends to wash out any resonance peaks. Indeed we see some suggestive evidence for  $K^*$  in our data, but the limited statistics and, we suspect, the suppression effect just mentioned, make it difficult to draw definitive conclusions.

Furthermore, the absence in Table I of any entry for the three-body final states  $\Lambda K^+ \pi^-$  and  $\Lambda K^0 \pi^0$  signifies the relative dearth of such events. (They constitute approximately 1% of the total  $\Lambda$  production.) It would be difficult, offhand, to understand this result on the basis of an intrinsic three-body annihilation mechanism. However, the double-scattering mechanisms of Fig. 2 give a natural explanation, since either of the processes shown has a strong probability of producing multiple pions.

#### IV. TEST OF ISOSPIN INVARIANCE

The  $\bar{p}d$  final states reported here provide a simple and convenient test of isotopic spin invariance by means of the Lipkin-Peshkin relations.<sup>8</sup> For  $\bar{p}d$  interactions leading to all possible charge combinations of any fixed set of final particles, as well as for inclusive processes, one obtains relations between the average multiplicities of charged and neutral pions, and between the average total energies carried by charged and neutral pions:

$$\langle n_{\pi^+} \rangle + \langle n_{\pi^-} \rangle = 2 \langle n_{\pi^0} \rangle, \quad (6)$$

$$\langle E_{\pi^+} \rangle + \langle E_{\pi^-} \rangle = 2 \langle E_{\pi^0} \rangle. \quad (7)$$

A significant deviation from the second relation was reported<sup>9</sup> in the process  $\bar{p}d \rightarrow$  pions + nucleon at rest. This deviation is, to our knowledge, unconfirmed at this time. It is potentially important owing to an interpretation<sup>10</sup> in terms of excess  $\gamma$  production possibly associated with radiative decays of baryonium states.

We have considered the isospin relations as they apply to the process  $\bar{p}d \rightarrow \Lambda + \text{anything}$ . Due to the impossibility of disentangling multi- $\pi^0$  final states the mean multiplicity relation (6) is not very useful. It can be applied unambiguously to the  $\Lambda K\pi$  final state, but there are too few events to yield a significant result. An unambiguous and statistically significant result can, however, be obtained for a test of the energy relation (7). For this test we use only events containing a  $K^+$  or a visible  $K^0$ , in which case the total energies carried by charged or neutral pions can be determined from fits or missing energy calculations. All charged particles in these events are identified by ionization. Due to the relatively low average momenta of the kaons, the separation from pions is quite clear and the particle identifications are essentially unambiguous.  $K^0$  events are weighted to correct for neutral decay modes and scanning inefficiency. Combining all topologies at each beam momentum in order to achieve maximum statistical accuracy, we obtain for the ratio of total charged to total neutral energy the values shown in Table II.

The results show a systematic deviation from the 2:1 ratio predicted on the assumption of isospin in-

variance. An average of the results yields the value  $1.77 \pm 0.05$ . The discrepancy corresponds to an average excess of approximately 30 MeV in the total neutral pion energy. Some deviation from isospin invariance in this direction can be explained naturally if the final states contain  $\eta$  and/or  $\omega$  production, since electromagnetic decays of these particles will tend to enhance the energy going into neutrals ( $\gamma$ 's as well as  $\pi^0$ 's). A detailed calculation of this effect is difficult without information on the average energy carried by an  $\eta$  or  $\omega$  in the final state. Based on an estimate of this energy, and using the known decay branching ratios, we estimate that the entire observed isospin violation could be explained by approximately 8%  $\eta$  production, or 60%  $\omega$  production, or some linear combination of the two.

Effective-mass distributions for  $\pi^+\pi^-\pi^0$  in fitted events show a clear  $\omega$  and a suggestion of possible  $\eta$  production. We estimate the  $\omega$  production in the sample used for the isospin test (including unfitted events) to be on the order of 10% with an absolute upper limit of  $\sim 25\%$ . The  $\eta$  production situation is less clear; however, we find we cannot exclude the possibility of as much as 6% or even more. Hence the entire effect of a charged to neutral energy ratio of 1.77 is not inconsistent with isospin violation arising purely from  $\eta$  and  $\omega$  decays. If this number were moved closer to 2 by one or two standard deviations, the effect would be readily understandable. The observed isospin violation appears to require no exotic explanation.

#### V. CONCLUSIONS

The reaction  $\bar{p}d \rightarrow \Lambda + \text{anything}$  below 1 GeV/c is consistent with a double-scattering mechanism in which a  $\bar{K}$  is exchanged as shown in Fig. 2(b). The observations that (i) the  $\Lambda$  angular distribution does not exhibit peripheral behavior, (ii) the peak in the missing mass recoiling off the  $\Lambda$  is explainable by phase space, and (iii) the cross section is exceptionally large tend to rule out the  $\bar{\Lambda}$  exchange mechanism. The estimated rate for  $\Lambda$  production as a result of a  $\bar{K}$  exchanged between the two vertices is in agreement with our data. The data are also found to disagree with a rigorous prediction from isospin invariance for the ratio of energies carried by charged

TABLE II. Ratio of total energies of charged and neutral pions.

$P_{\text{beam}}(\text{MeV}/c)$	ANL experiment			BNL experiment		
	300-550	550-650	650-725	552	740	905
$\frac{\langle E_{\pi^+} \rangle + \langle E_{\pi^-} \rangle}{\langle E_{\pi^0} \rangle}$	$1.83 \pm 0.18$	$1.62 \pm 0.15$	$1.69 \pm 0.13$	$2.18 \pm 0.15$	$1.85 \pm 0.10$	$1.68 \pm 0.08$

and neutral pions. However, this effect appears to be consistent with the deviation expected due to  $\omega$  and  $\eta$  mesons in the final state.

#### ACKNOWLEDGMENTS

We wish to acknowledge the contributions made by the BNL Alternating Gradient Synchrotron and ANL Zero Gradient Synchrotron staffs and bubble-chamber crews during the course of the experiment, as well as the assistance of the UCI scanning group, in particular Coleen Cory who supervised the scanning operation. We also wish to thank Barbara Billiris for her contribution to writing the software for our scanning-table operating system. This work was performed under the auspices of the U.S. Department of Energy.

#### APPENDIX A: $\bar{\Lambda}$ -EXCHANGE CALCULATION

The double-scattering mechanism involving  $\bar{\Lambda}$  exchange was calculated from the triangle diagram of Fig. 2(a), using the following approximations and assumptions.

$$d\sigma \cong \frac{\alpha}{4\pi^2} \frac{n(n+1)}{(n-1)^2} (X^2 + Y^2) \frac{(E_B - m)^2 m_B}{p_B^2 E_B} \frac{d\sigma_A}{dp_{\bar{\Lambda}}} v_{(B)} d\sigma_B dp_B dm_B. \quad (\text{A1})$$

Here  $d\sigma_A/dp_{\bar{\Lambda}}$  is the differential cross section for producing  $\bar{\Lambda}$  at the  $A$  vertex,  $v_{(B)}d\sigma_B$  is essentially the flux times differential cross section, i.e., rate, for the  $B$  vertex process at c.m. energy  $m_B$ , and

$$X \equiv \tan^{-1} \left[ \frac{(n-1)\lambda}{1+n\lambda^2} \right],$$

$$Y \equiv \frac{1}{2} \ln \left[ \frac{1+n^2\lambda^2}{1+\lambda^2} \right],$$

where

$$\lambda \equiv \frac{2\alpha p_B}{|(m_B - m)^2 - m_{\Lambda}^2 - 2m(E_B - m_B)|}.$$

(1) The dominant term corresponding to deuteron dissociation is retained, and the resulting pole term and vertex function are replaced by a momentum-space wave function of the Hulthen form

$$\psi(k) \propto \left[ \frac{1}{k^2 + \alpha^2} - \frac{1}{k^2 + n^2\alpha^2} \right],$$

where  $\alpha = \sqrt{mB}$ ,  $m$  is the nucleon mass,  $B$  is the deuteron binding energy, and  $n$  is a numerical constant ( $\approx 5.5$ ).

(2) The exchanged  $\bar{\Lambda}$  is treated effectively as a particle with variable mass, and off-shell amplitudes are approximated by measured on-shell results.

(3) Spins are ignored, and nonrelativistic kinematic approximations are made wherever possible.

(4) To obtain numerical results we use  $\sigma_{\bar{p}p}$  (annihilation) as an estimate of the unmeasured  $\sigma_{\bar{\Lambda}N}$  (annihilation).

The final result gives for the differential cross section as function of the laboratory momentum  $p_B$  and effective mass  $m_B$  of the particles produced at the  $B$  vertex:

Treating the initial nucleon at the  $B$  vertex as essentially at rest in the laboratory, then  $p_{\bar{\Lambda}} \approx p_B$ . The functional form of  $d\sigma_A/dp_{\bar{\Lambda}}$  can be obtained from the observed peripheral behavior of the process  $\bar{p}p \rightarrow \bar{\Lambda}\Lambda$  for which  $d\sigma/dt \propto e^{-bt}$ .

Finally, the total rate,  $\int v_{(B)}d\sigma_B$ , for the  $\bar{\Lambda}N$  annihilation at the  $B$  vertex can be estimated from the typical low-energy  $1/v$  capture-cross-section behavior, using  $\bar{p}p$  annihilation as a model, for which  $\int v d\sigma \approx 60$  mb.

Integrating the result (A1) over  $p_B$  gives the form of the differential cross section  $d\sigma/dm_B$  plotted in Fig. 3 (distribution normalized to the number of events); further integration gives the cross-section result plotted in Fig. 1.

<sup>1</sup>R. Bizzarri *et al.*, Lett. Nuovo Cimento **2**, 431 (1969).

<sup>2</sup>U. Camerini *et al.*, Nucl. Phys. **B33**, 505 (1971).

<sup>3</sup>B. Y. Oh and G. A. Smith, Nucl. Phys. **B40**, 151 (1972).

<sup>4</sup>G. Lynch, Rev. Mod. Phys. **33**, 395 (1961).

<sup>5</sup>L. N. Bogdanova and V. E. Markushin, Yad. Fiz. **28**, 1390 (1978) [Sov. J. Nucl. Phys. **28**, 715 (1978)].

<sup>6</sup>T. S. Mast *et al.*, Phys. Rev. D **11**, 3078 (1975).

<sup>7</sup>N. Dean, Phys. Rev. Lett. **27**, 276 (1971).

<sup>8</sup>H. J. Lipkin and M. Peshkin, Phys. Rev. Lett. **28**, 862 (1972); M. Peshkin, Phys. Rev. **121**, 636 (1961).

<sup>9</sup>T. E. Kalogeropoulos *et al.*, Phys. Rev. Lett. **33**, 1631 (1974).

<sup>10</sup>T. E. Kalogeropoulos *et al.*, Phys. Rev. Lett. **33**, 1635 (1974).